Variational phasespace theory studies of siliconatom diffusion on reconstructed Si(111)(7×7) surfaces

Paras M. Agrawal, Donald L. Thompson, and Lionel M. Raff

Citation: The Journal of Chemical Physics **91**, 6463 (1989); doi: 10.1063/1.457362
View online: http://dx.doi.org/10.1063/1.457362
View Table of Contents: http://scitation.aip.org/content/aip/journal/jcp/91/10?ver=pdfcov
Published by the AIP Publishing

Variational phase-space theory studies of silicon-atom diffusion on reconstructed Si(111)-(7×7) surfaces

Paras M. Agrawal, Donald L. Thompson, and Lionel M. Raff
Department of Chemistry, Oklahoma State University, Stillwater, Oklahoma 74078

(Received 8 June 1989; accepted 10 August 1989)

The dynamics of silicon-atom diffusion on a reconstructed Si(111)-(7×7) surface have been investigated using variational phase-space theory methods with a previously described [J. Chem. Phys. (to be published)] potential-energy surface. A four-layer lattice model of the Binnig *et al.* (7×7) reconstruction containing 291 atoms is employed for the surface. Canonical Markov walks with importance sampling incorporated are used to evaluate the flux across both right-circular and right-elliptical cylindrical dividing surfaces separating adsorption sites. This flux is minimized with respect to the parameters of the dividing surface to obtain the best estimate of the classical jump frequencies. The minimum jump frequencies so obtained are corrected for recrossings of the dividing surface by the calculation of trajectories that start from phase-space points obtained in the random walk that lie within a specified distance w of the dividing surface. The corrected jump frequencies are then used as input to a set of 225 diffential equations that describe the diffusion rates across the (7×7) surface. Diffusion coefficients D are computed from the slope of plots of the time variation of the root-mean-square displacements obtained from the solution of the rate equations. Arrhenius plots of results obtained at 300, 600, and 1000 K yield $D = 2.15\times10^{-3}\exp(-1.51\ \text{eV}/k_BT)\ \text{cm}^2/\text{s}$. The calculated activation energy of 1.51 eV is in excellent accord with the result obtained by Farrow from molecular-beam pyrolysis data on SiH_4 deposition. An examination of the details of the diffusion shows that it is not isotropic on the (7×7) surface. We find that preferential directions of flow exist. These directions correspond to "gateways" at three of the four corners of the (7×7) unit cell. The results suggest that diffusion rates are a sensitive function of the geometry of the (7×7) reconstruction so that careful measurements of diffusion rates and associated activation energies may be able to serve as a means of differentiating different proposed models of the Si(111)-(7×7) reconstruction.

I. INTRODUCTION

The chemical-vapor deposition (CVD) of silicon from silane is comprised of many elementary steps. The important heterogeneous processes involve collisions of SiH_4, SiH_2, and Si_n ($n = 1,2,3,...$) clusters with a silicon surface followed by chemisorption and surface reaction of these species. We have recently reported theoretical studies of such processes for SiH_2 on Si(111) and reconstructed Si(111)-(7×7) surfaces.[1,2] Once gaseous silicon atoms are chemisorbed on the surface either by direct adsorption of Si(g) or by formation via decomposition reactions of SiH_4, SiH_2, or Si_n, there are two additional competitive processes that require consideration.[3,4] The first of these is the desorption rate which is of central importance in the interpretation of film-growth experiments. The second is the diffusion of the chemisorbed atoms over the surface which may lead to attachment at a stable kink point and further film growth. Surface diffusion is also important in many other surface phenomena such as heterogeneous crystal catalysis, epitaxial growth, sintering, and corrosion. Consequently, this has been a subject of growing interest in recent years.[3–14]

Doll and co-workers[15] have applied molecular-dynamics and transition-state theory methods to investigate surface diffusion for fcc and bcc systems. Banavar, Cohen, and Gromer[16] have used the Fokker–Planck formalism to examine diffusion of various adsorbates on tungsten. Tully, Gilmer, and Shugard[13] introduced a "ghost" atom approach to compute diffusion rates. More recent work has focused upon the contribution of tunneling in surface diffusion and upon methods that permit the effect of the surface-phonon modes to be included in the calculations.[14,17–19] The diffusion of silicon on unreconstructed Si(111)-(1×1) and on Si(100) surfaces has been investigated in our laboratory using classical trajectory methods.[5–7] Takai, Halicioglu, and Tiller[8] computed the activation energy for surface diffusion of silicon over Si(111) using contour maps of a semiempirical potential-energy surface.

Our previous silicon diffusion studies[6] gave an activation energy for diffusion on Si(111)-(1×1) that was in good accord with results obtained from direct deposition experiments[11] but much lower than other data from molecular-beam-pyrolysis experiments.[9,10,12] These results suggest that the direct deposition measurements[11] were monitoring diffusion on a terrace whereas the molecular-beam experiments were seeing diffusion on surfaces containing kinks and/or dislocations. However, in the temperature range of interest, the Si(111)-(1×1) surface undergoes reconstruction to form Si(111)-(7×7). Since diffusion on Si(111)-(1×1) may be very different from that on the Si(111)-(7×7) reconstruction, the direct comparison of our previous results[6] with experimental data[9–12] may be inappropriate.

The present paper reports the results of variational phase-space calculations of silicon-atom diffusion rates on

Si(111)-(7×7). Such studies will permit a more accurate comparison with the available experimental data and may be helpful in the determination of a better potential-energy surface. The exact nature of the (7×7) reconstruction is unknown and the results may shed additional light on this question.

The variational phase-space method used here has recently been used in a study of the diffusion of hydrogen atoms on a Si(111) surface partially covered by hydrogen.[14] In Sec. II, the formulation of the method is reviewed and the results are given and discussed in Sec. III.

II. METHODS

A. Lattice model and diffusion equations

For the Si(111)-(7×7) reconstructed surface we employ the model structure given by Binnig *et al.*[20] In this model, there are 25 dangling bonds per unit cell, 12 in the top layer and 13 in the second layer. A modified Keating potential[21] is used to describe the lattice interactions. This lattice model, its relaxation energy, and geometry are fully described in Ref. 2. Figure 1 shows a top view of nine unit cells of the (7×7) Binnig *et al.* lattice. The octagonals and diamonds represent the first- and second-layer sites with dangling bonds, respectively.

Starting from an adatom chemisorbed at the lattice site denoted by "*A*" in Fig. 1, we consider the diffusion to the other 224 lattice sites with dangling bonds shown in the figure. The diffusion coefficient D is computed form the mean-square displacement from site A:

$$\langle r^2(t)\rangle = 2\alpha D t , \tag{1}$$

where α is the dimensionality of the diffusion and

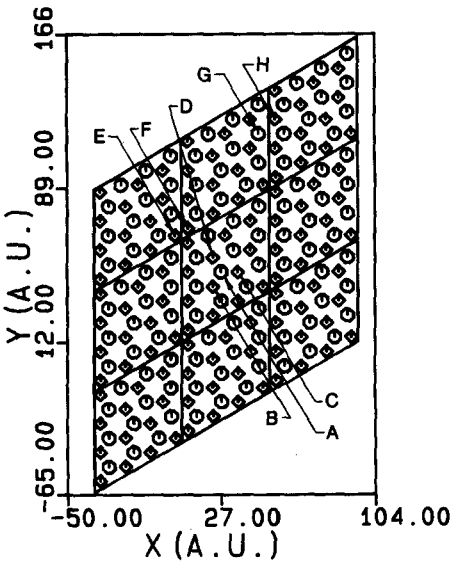

FIG. 1. Unrelaxed XY coordinates of 225 atoms with dangling bonds in nine unit cells of the Si(111)-(7×7) reconstructed surface model suggested by Binnig *et al.* Octagonals denote the 108 atoms in the top layer ($Z=0$) and the diamonds represent the 117 atoms in the second layer ($Z=-1.48$ a.u.).

$$\langle r^2(t)\rangle = \sum_{i=1}^{N} [C_i(t) r_i^2(t)] \Big/ \sum_{i=1}^{N} [C_i(t)] . \tag{2}$$

In these equations, t is the time, $C_i(t)$ is the concentration of diffusing adatoms at time t at the ith site which is at distance r_i from site A, and N is the total number of such sites considered. In the present calculation, we have taken $N=225$. At $t=0$, we take $C_i(0)=0$ for $i\neq A$. The $C_i(t)$ are obtained from the solution to the following set of coupled differential equations:[6]

$$\dot{C}_i(t) = \sum_{j=1}^{N}{}' (-K_{ij}C_i + K_{ji}C_j) \quad (i=1,2,3,...,N) . \tag{3}$$

Here, K_{ij} is the jump frequency from site i to site j.

These equations are based upon the phenomenological process of diffusion together with the assumption that the adatoms experience such a high barrier to diffusion that each diffusion jump is totally uncorrelated with previous jumps. Such an assumption will be reasonable if the characteristic time for diffusion, given by the inverse of K_{ij}, is much larger than the vibrational relaxation time that may be on the order of 1000 vibrational periods. The results given in the text section show that this condition is satisfied for the present system.

The individual K_{ij} are obtained by first computing K_i, where

$$K_i = \sum_j K_{ij} , \tag{4}$$

using the Monte Carlo variational phase-space method described below. The K_{ij} are then obtained by symmetry considerations. That is, the jump frequency from site A to B, K_{A-B}, would be almost equal to $K_A/3$ due to the symmetry of sites B, C, and D about site A and due to the fact that the jump frequencies to all other distant sites will be very small compared to K_{A-B}. For the Binnig *et al.* model of the (7×7) reconstruction, the results show that the diffusion coefficient is insensitive to jump frequencies between sites other than those equivalent to those involved in the calculation of K_A.

B. Variational phase-space methods

The required jump frequencies are obtained using a modified version of the variational phase-space theory approach we have previously employed to study the diffusion of hydrogen atoms on a Si(111)-(1×1) surface with partial hydrogen coverage.[14] These methods are based on ideas described by Keck.[22] Similar procedures have been devised by others to treat a wide variety of homogeneous and heterogeneous processes. The framework in which we use the theory is described below.

Consider the migration of a silicon atom from a site A, which we will denote by $*'$. This migration can be represented by

$$*'\text{–Si} + *'' \rightarrow *' + *''\text{–Si}. \tag{5}$$

Here $*''$ denotes a site other than $*'$ on the surface having a dangling bond. In principle, there exists a closed dividing surface S_a that encloses the volume Ω_a in phase space such that $*'$ lies inside this volume. If, at some moment, the ada-

tom is found to lie outside this surface, we may say that the silicon atom has migrated from site $*'$. This concept can be used in conjuction with the hydrodynamical equation of continuity to compute the number of states inside the volume Ω_a and the related flux crossing the surface S_a to evaluate the rate of reaction (5).

Consider an ensemble of systems each containing n classical particles. The state of each system can be represented by a point in $6n$-dimensional phase space. Let ρ be the density of such representative points. Since the number of points is conserved, ρ satisfies the equation

$$\frac{d\rho}{dt} + \mathrm{div}(\rho \mathbf{v}) = 0, \tag{6}$$

where $\mathbf{v}$ is the generalized velocity in $6n$-dimensional phase space and likewise the divergence and density refer to the generalized quantities in the phase space. The components of the velocity can be obtained from Hamilton's equations of motion using the Hamiltonian, H, for the n-particle system. Integration of Eq. (6) over the volume Ω_a gives

$$-\frac{dN_a}{dt} = \int_{\Omega_a} \mathrm{div}(\rho \mathbf{v}) d\Omega = \int_{S_a} \rho \mathbf{v} \cdot d\mathbf{S}, \tag{7}$$

where

$$N_a = \int_{\Omega_a} \rho \, d\Omega \tag{8}$$

is the number of systems in the ensemble which are in state $*'$–Si.

The surface integral in Eq. (7) can be separated into two parts: one representing the outgoing flux for which $\mathbf{v}\cdot d\mathbf{S}$ is positive, and other describing the incoming flux for which $\mathbf{v}\cdot d\mathbf{S}$ is negative. That is, we may write

$$-\frac{dN_a}{dt} = \int_{S_a} I_{\mathrm{out}} \rho \mathbf{v} \cdot d\mathbf{S} + \int_{S_a} I_{\mathrm{in}} \rho \mathbf{v} \cdot d\mathbf{S}, \tag{9}$$

where

$$I_{\mathrm{out}} = \begin{cases} +1 & \text{for } \mathbf{v}\cdot d\mathbf{S} > 0, \\ 0 & \text{otherwise} \end{cases},$$

$$I_{\mathrm{in}} = \begin{cases} +1 & \text{for } \mathbf{v}\cdot d\mathbf{S} < 0, \\ 0 & \text{otherwise.} \end{cases}$$

Under equilibrium conditions, the incoming flux given by the second term on the right-hand side (RHS) of Eq. (9) will be equal in magnitude to the outgoing flux given by the first term. The number of systems undergoing reaction (5) per unit time would therefore be given by the first term on the RHS of Eq. (9), and the corresponding rate of reaction of (5) would be

$$K = \int_{S_a} I_{\mathrm{out}} \rho \mathbf{v} \cdot d\mathbf{S} / N_a = \int_{S_a} I_{\mathrm{out}} \rho \mathbf{v} \cdot d\mathbf{S} \Big/ \int_{\Omega_a} \rho \, d\Omega . \tag{10}$$

We now assume that the internal degrees of freedom of the reactants are in local equilibrium and can therefore be described by a Boltzmann distribution,

$$\rho = \rho_0 \exp(-\beta H), \tag{11}$$

where $\beta = (k_B T)^{-1}$ with k_b being Boltzmann's constant and T the surface temperature. Combination of Eqs. (10) and (11) gives

$$K = \int_{S_a} I_{\mathrm{out}} \exp(-\beta H) \mathbf{v} \cdot d\mathbf{S} \Big/ \int_{\Omega_a} \exp(-\beta H) d\Omega . \tag{12}$$

Let V_{La} be the interaction between the lattice and the adatom. We define

$$H' = H - V_{La} . \tag{13}$$

Substitution of Eq. (13) into Eq. (12) yields

$$K = \int_{S_a} I_{\mathrm{out}} \exp(-\beta V_{La}) \exp(-\beta H') \mathbf{v} \cdot d\mathbf{S} \times \left[\int_{\Omega_a} \exp(-\beta V_{La}) \exp(-\beta H') d\Omega \right]^{-1} . \tag{14}$$

The computation of K using Eq. (14) requires knowledge of the dividing surface S_a in the phase space that separates the reactants and products of reaction (5). The ideal surface would be such that trajectories cross once and only once in going from the reactant phase space to that of the products. For any other dividing surface, K will be an upper limit to the true classical rate. In the present variational method, the flux given by Eq. (14) is minimized with respect to the parameters present in a trial dividing surface.

The velocity, volume, and surface in Eq. (14) refer to those in $6n$-dimensional phase space. However, for diffusion reactions such as (5), the best dividing surface may be a rather insensitive function of the coordinates and momentum of the Si(111)-(7×7) lattice atoms. We have therefore assumed that the quantities in Eq. (14) are functions of the adatom coordinates only.

The integrals in Eq. (14) are evaluated using standard Monte Carlo procedures with importance sampling. The Monte Carlo approximant for K is

$$K = (F/2w) \sum_j I_j'(S_a, w) \, |v_p| (P_0^{-1}) \Big/ \sum_j I_j'(\Omega_a) (P_0^{-1}) . \tag{15}$$

In Eq. (15), j refers to the jth accepted move in a canonical Markov walk, $P_0 = \exp(\beta V_{La})$, and $|v_p|$ is the magnitude of $\mathbf{v}\cdot d\mathbf{S}$, i.e., the magnitude of the component of the velocity of the adatom "perpendicular" to the dividing surface S_a. $I_j'(S_a, w)$ is an operator that has value $+1$ if, by the jth move, the adatom is within the volume bounded by surfaces S_a and S_a', where S_a' is a surface very close and parallel to S_a at a distance of w from S_a; otherwise $I_j'(S_a, w)$ is equal to zero. The operator $I_j'(\Omega_a)$ is equal to $+1$ if the jth move leads to a state such that the adatom is inside the volume Ω_a enclosed by the surface S_a. It is zero otherwise. F is a dynamical correction factor described below. The surface integral in Eq. (14) includes all terms with $\mathbf{v}\cdot d\mathbf{S} = v_p$ as positive. As discussed above, the contribution of outgoing and incoming flux will be equal in magnitude. Hence, the statistical accuracy may be increased for a given Markov walk by combining the flux in both directions and dividing the result by a factor of 2.

The Markov walk is executed in Cartesian coordinates and their conjugate momenta by the usual presecription:

$$q_i' = q_i + (0.5 - \xi_1)\Delta q\,, \tag{16}$$

$$p_i' = p_i + (0.5 - \xi_2)\Delta p\,, \tag{17}$$

where Δq and Δp are the step-size parameters and ξ_1 and ξ_2 are random numbers whose distribution is uniform on the interval [0,1]. The silicon adatom and five lattice atoms are moved in each Markov step with the selection of the five moving lattice atoms being cycled systematically over all n movable lattice atoms. That is, if in the ith move, lattice atoms $j, j+1,...,j+4$ are used in the Markov walk, then in the $(i+1)$th move, lattice atoms $j+1, j+2,...,j+5$ will be used. After the Markov step in which lattice atoms $n-4$, $n-3,...,n$ are moved, the cycle returns to the first lattice atom and atoms $n-3$, $n-2,...,n,1$ are used in the subsequent step. In each move, the position and momentum of the fifth lattice atom are adjusted to ensure conservation of center-of-mass momentum. Markov moves are accepted if the position of the adatom lies within a reflecting surface located within distance w outside of S_a', and if

$$P''/P' > \xi_3, \tag{18}$$

where P'' and P' are the values of $\exp(-\beta H')$ after and before the move, respectively.[23]

Since the dividing surface has been assumed to be a function of the adatom coordinates only, and since there is a practical limit to the number of such dividing surfaces that can be investigated, the minimum flux obtained from Eq. (14) will include trajectories that recross S_a. This flux will therefore be an upper limit to the true classical rate coefficient. The factor F in Eq. (15) corrects for such recrossings.

Whenever the adatom crosses S_a, the positions and momenta of all atoms are recorded as members of a set $\{q,p\}$. After completion of the Markov walk, a random selection of M sets of $\{q,p\}$ is made. Classical trajectories are then calculated using each set $\{q,p\}$ as the initial conditions for a trajectory. The dynamical correction factor is then given by

$$F = \sum_{j=1}^{M} I_j |v_p|_j (P_0^{-1})_j \Big/ \sum_{j=1}^{M} |v_p|_j (P_0^{-1})_j\,, \tag{19}$$

where I_j is unity if trajectory j does not recross S_a and maps properly into the product and reactant configuration space; otherwise, I_j is zero.

III. RESULTS AND DISCUSSION

A. Jump frequencies

Equation (15) has been used to compute the jump frequency, K_A, between sites "A" and "B", and "C" and "D" in Fig. 1 at temperatures of 300, 600, and 1000 K. For these calculations, a four-layer lattice model containing 291 lattice atoms arranged in a manner consistent with the Si(111)-(7×7) model of Binnig *et al.* is used.[2,20] This set of 291 atoms has 12 and 26 atoms with dangling bonds in the first and second layers, respectively. The remaining 55, 99, and 99 atoms in the second, third, and fourth layers, respectively, do not have dangling bonds.

The interaction potential is the limiting form of that described in Ref. 2 for the SiH_2-Si(111)-(7×7) system. The present calculations take the limit of this potential as all Si–hydrogen distances approach infinity. The pairwise sums in this potential include the interaction of the adatom with all lattice atoms. The interaction between the adatom and lattice atoms with dangling bonds is assumed to have a Lennard–Jones (12,6) form while the interaction with closed-shell lattice atoms is taken to be the repulsive interaction obtained from the self-consistent-field (3-21G) calculations reported in Ref. 2. All potential parameters are as previously reported.[2]

The Markov walk parameters are $\Delta q = 0.10$ a.u. and $\Delta p = 0.10$ m.u. (1 m.u. $= 1.631\times10^{-18}$ cgs units). Only the 38 atoms of the lattice having dangling bonds are allowed to move during the Markov walk. Reflecting barriers are placed in the surface plane ($z = 0$) and at a distance 6.0 a.u. above and parallel to the surface plane. The adatom is not permitted to penetrate these barriers during the Markov walk. Convergence of the results is found to be satisfactory for walks of 2×10^6 steps at each temperature investigated.

We have utilized dividing surfaces identical to those previously employed in our studies of hydrogen-atom diffusion on partially-covered Si(111) surfaces.[14] These are for right circular cylinders:

$$x^2 + y^2 - a^2 = 0; \tag{20}$$

and for right elliptical cylinders:

$$x^2/a^2 + y^2/b^2 - 1 = 0. \tag{21}$$

In these equations, we take site A as the origin (see Fig. 1). The calculated jump frequencies have been minimized with respect to the a and b parameters by grid searches over the range 4.7 a.u. $\leqslant a$ and $b \leqslant 5.1$ a.u. for elliptical cylinders and $0.5 \leqslant a \leqslant 6.2$ a.u. for circular dividing surfaces. At $T = 1000$ K, the optimum circular dividing surface is obtained for $a = 4.9$ a. u. The optimum elliptical surface has $a = 5.0$ a.u. and $b = 4.7$ a.u. As expected, lower fluxes are obtained with S_a defined by Eq. (21).

The correction factor at $T = 1000$ K for recrossing has been obtained by the computation of 175 trajectories as described above. The result is $F = 0.335$. This value has been assumed to be insensitive to the temperature over the range investigated in the present study. The values of K_A at 300, 600, and 1000 K obtained from Eq. (15) are given in Table I. An Arrhenius plot of these results is shown in Fig. 2. The slope and intercept of the least-squares fit gives an activation energy of 1.51 eV and a frequency factor of $0.734\times10^{13}\ s^{-1}$.

Figure 3 shows the minimum-energy diffusion path from site $*'$ to $*''$ obtained by methods previously described by Raff, NoorBatcha, and Thompson.[24] The points correspond to the minimum potential-energy configuration observed in the Markov walk at right circular cylindrical divid-

TABLE I. Jump frequencies K_A for reaction (5) and the diffusion coefficient D in cgs units as a function of the surface temperature T in degrees Kelvin.

T	K_A	D
300.0	0.274×10^{-12}	0.854×10^{-28}
600.0	0.161×10^{1}	0.483×10^{-15}
1000.0	0.161×10^{6}	0.482×10^{-10}

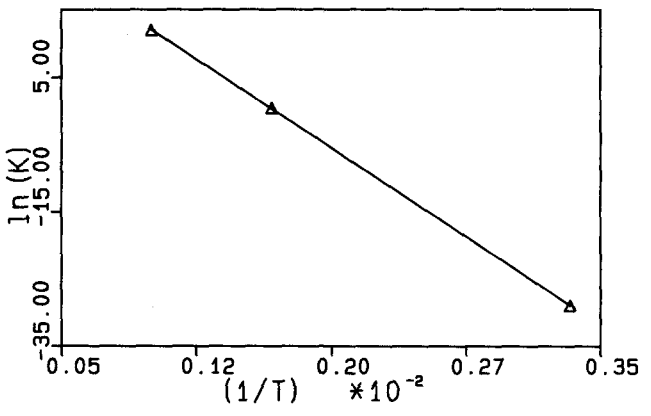

FIG. 2. $\ln(K)$ vs $1/T$ in degrees Kelvin. K is the jump frequency for reaction (5) in units of 1/s. The triangles are the computed points and the straight line is a least-squares fit.

ing surfaces set at intervals along the reaction path. The abscissa values of the points in the figure correspond to the radii of the dividing surfaces and the ordinate to the minimum value of the potential obtained on that dividing surface. The result gives a barrier height for reaction (5) of 1.61 eV, in agreement with the activation energy of 1.51 eV obtained from the temperature dependence of the calculated jump frequencies. The difference of 0.1 eV may be due to use of the circular cylinders to obtain the data in Fig. 3 instead of the elliptical cylinders used to compute K. Statistical errors may also account for some of this difference.

B. Diffusion coefficients

The calculation of the diffusion coefficient from Eqs. (1)–(3) requires all of the K_{ij} as input. In all of the diffusion calculations, the set of 225 differential equations represented by Eq. (3) was solved using an Adams–Moulton method with variable step size.

An examination of Fig. 1 shows that the different pairs of atoms with dangling bonds can be broadly classified into four groups.

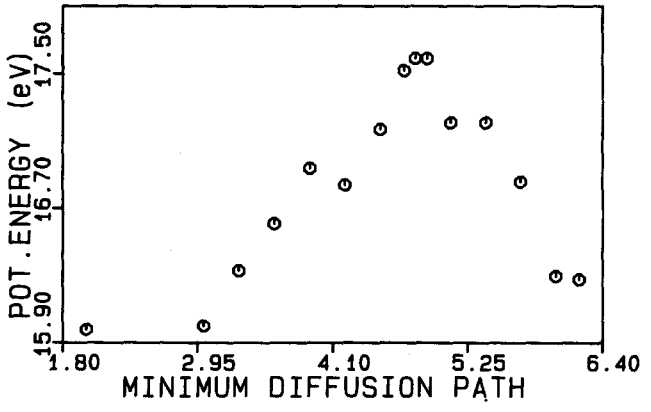

FIG. 3. Minimum potential-energy path for silicon-atom jumps from site A of Fig. 1 to a neighboring site. The abscissa shows the radius in a.u. of the circular dividing surfaces having point A (see Fig. 1) as the origin.

(1) Diffusion from site A to site B, C, or D, i.e., diffusion from an atom to a neighboring site which is at a distance of about 8.5 a.u. The jump frequency K_{ij} for such a pair can be taken to be $K_A/3$. We may also assume that $K_{ij} = K_{ji}$ since the adsorption energy at all bonding sites is approximately the same.

(2) Diffusion from sites such as E to sites like F (see Fig. 1) which are at a distance of about 7.3 a.u. We would expect K_E for such jumps to be larger than K_A due to a lower barrier height associated with the closer proximity of the sites.

(3) Jumps from sites such as G to sites like H, i.e., pairs at a distance of about 11.2 a.u. For such a pair, the jump frequency will be much less than K_A.

(4) Jumps over distances more than 11.2 a.u. The jump frequencies associated with such events can be taken to be zero without significant loss of accuracy.

An inspection of the geometry of the (7×7) lattice shown in Fig. 1 suggests that the diffusion coefficient will not be sensitive to the values of K_E or K_G. The exact value of the larger jump frequency between sites E and F will not be rate determining because of the slower jump rates between other sites. The lower rate K_G cannot significantly limit the overall diffusion rate due to the fact that alternative routes with higher jump frequencies are available for diffusion over a large distance. These intuitive observations are supported by sensitivity studies of the diffusion coefficient to K_E and K_G. Table II shows the variation of the diffusion coefficient D for various values of K_E and K_G spanning a wide range. The insensitivity of D to K_E and K_G is clearly evident. D increases 2% with the increase of K_E by a factor of 20 and by 10% for a 100-fold increase in K_G. We expect the value of K_G to be lower than the maximum value considered in Table II. Consequently, the difference in the value of D computed using $K_E = 100\times(K_A/3)$ and $K_G = (K_A/3)/1000$ and that using the exact but unknown values of K_G and K_E is expected to correspond to less than a 10% variation.

Diffusion coefficients have been obtained using Eq. (1), which predicts that the mean-square displacement will be a linear function of time. Figure 4 shows a typical result. The slight departure from linearity at large values of time is due to edge effects from the nine unit cells over which the diffusion is followed. Diffusion coefficients obtained from the slopes of mean-square displacement plots at 300, 600, and 1000 K with $K_E = 100(K_A/3)$ and $K_G = (K_A/3)/1000$ are given in Table I. An Arrhenius plot of these results is shown in Fig. 5. The linearity is excellent. The intercept and slope yield a preexponential factor of 2.15×10^{-3} cm^2/s and an

TABLE II. Diffusion coefficients D in cgs units as a function of jump frequencies at a surface temperature of 1000 K.

$K_E/(K_A/3)$	$(K_A/3)/K_G$	D
5.0	1000.0	0.472×10^{-10}
10.0	1000.0	0.478×10^{-10}
50.0	1000.0	0.480×10^{-10}
100.0	1000.0	0.482×10^{-10}
100.0	100.0	0.484×10^{-10}
100.0	10.0	0.536×10^{-10}

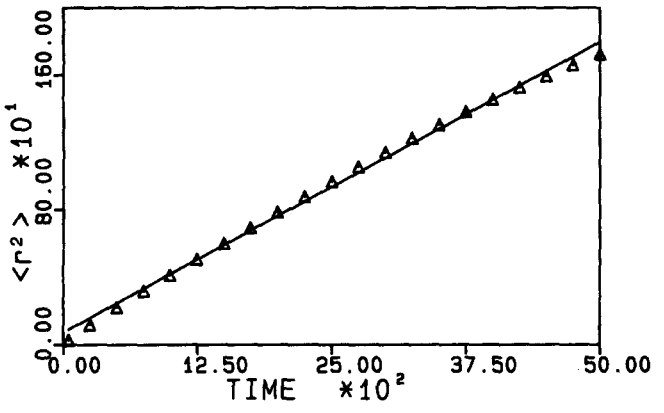

FIG. 4. $\langle r^2 \rangle$ in a.u.^{2} given by Eq. (1) as a function of time t in units of 0.5×10^{-7} s. The triangles are the computed points and the straight line is the least-squares fit.

activation energy of 1.51 eV. This activation energy is in excellent agreement with the value obtained by Farrow[9] from molecular-beam-pyrolysis experiments on SiH_4. It is 0.22 eV lower than the lower limit reported by Joyce, Bradley, and Booker[12] and 0.47 eV higher than the result obtained by Henderson and Helm.[10] The 0.2 eV activation energy obtained by Abbink, Broudy, and McCarthy[11] from the results of their direct deposition experiments seems much too low.

The activation energy obtained for silicon-atom diffusion on the (7×7) reconstruction is significantly larger than the 0.105 eV result we have previously calculated for the Si(111)-(1×1) surface.[6] Although there exist some differences in the potential-surface parameters used in the two studies, the major reason for the larger activation energy on the (7×7) surface is greater distance between adsorption sites on the reconstructed surface relative to that for Si(111)-(1×1). We now regard our comparison of diffusion results obtained on the unreconstructed surface with data obtained on the (7×7) reconstruction as inappropriate.

An inspection of the (7×7) lattice shown in Fig. 1 shows that the unit cell lacks reflection symmetry with respect to the short diagonal of the unit cell. This lack of symmetry leads to preferential directions for diffusion on the (7×7) surface. Figures 6(a) and 6(b) illustrate the nature of the diffusion process on the Binnig *et al.* (7×7) surface. In these perspective plots, the lattice surface is shown in the (x-y) plane, while the relative concentration of diffusing silicon atoms is shown along the z-axis. Each figure corresponds to a different time in the diffusion of silicon atoms at 1000 K, where all of the silicon-atom concentration is initially located at site A. It is clear that diffusion is not isotropic on this surface. It occurs primarily via "gateways" located at the three corners of the (7×7) unit cell which permit jumps of the type $E \rightarrow F$. Thus, while the magnitude of the diffusion coefficient is insensitive to the precise value of K_E, the fact that this jump frequency is significantly larger than that for all other jumps between adjacent sites causes the overall diffusion pattern to exhibit preferential directions of flow. This situation is analogous to that existing in a series of consecutive chemical reactions in which the final products are controlled by the fast steps, but the rate of production of those products is determined by the slow steps.

The angular dependence of the diffusion can be expressed conveniently by defining a quantity $d(\theta,t)$, the directional diffusion distance (DDD):

$$d(\theta,t) = \left[\frac{(1/2\Delta\theta) \sum_{\theta-\Delta\theta}^{\theta+\Delta\theta} C_i(\theta_i,t) r_i^2(\theta_i,t)}{(1/2\pi) \sum_{\theta=0}^{2\pi} C_i(\theta_i,t)} \right]^{1/2} . \quad (22)$$

Here, θ_i is the value of the angle for the ith lattice atom and $r_i(\theta_i,t)$ and $C_i(\theta_i,t)$ are, respectively, $r_i(t)$ and $C_i(t)$ defined in Eq. (2). Figure 7 shows polar plots of $d(\theta,t)$ at 1000 and 5000 t.u. (1 t.u. $= 0.5\times10^{-7}$ s) that illustrate the diffusion distance in different directions. That is, the position of point P in this figure shows that in time of 5000 t.u., the diffusing silicon atom, which was at point A at $t=0$, has diffused the distance AP in the direction **AP**. The propensity for the diffusion to occur along the three "gateways" is evident as is the restricted nature of the flow in the direction of the unit-cell corner that does not possess a "gate."

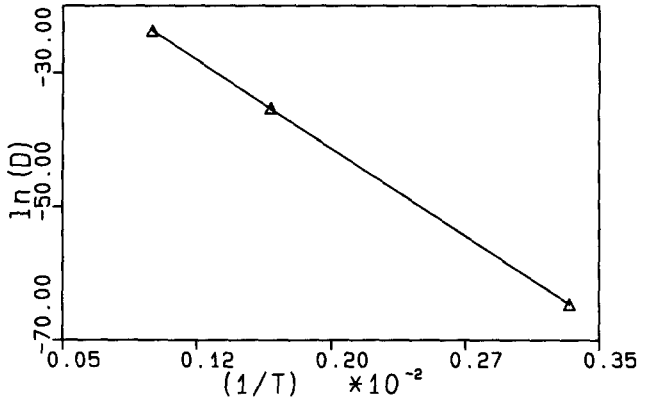

FIG. 5. ln(D) vs $1/T$ in degrees Kelvin. The diffusion coefficient D is in cm^2/s. The triangles are the computed points and the straight line is the least-squares fit.

C. Accuracy and sensitivity

The present potential-energy surface and the model of the Si(111)-(7×7) lattice give $K_A = 7.34\times10^{12} \times\exp(-1.51\ \text{eV}/k_BT)\ \text{s}^{-1}$. The preexponential factor is in good accord with the Si–Si–Si bending frequency given by the potential employed. The activation energy obtained from the temperature dependence of both K_A and D are in agreement. There is also near agreement between the calculated minimum barrier height for reaction (5) and the activation energy. The results are therefore internally consistent.

The degree of accuracy of the results relative to an experimental system depends upon the accuracy of the empirical potential-energy surface and also upon the sensitivity of the jump frequencies and of D to the potential parameters. We would expect the preexponential factor to change with variation in the Si–Si–Si bending frequency since diffusion across the surface necessarily involves this bending motion.

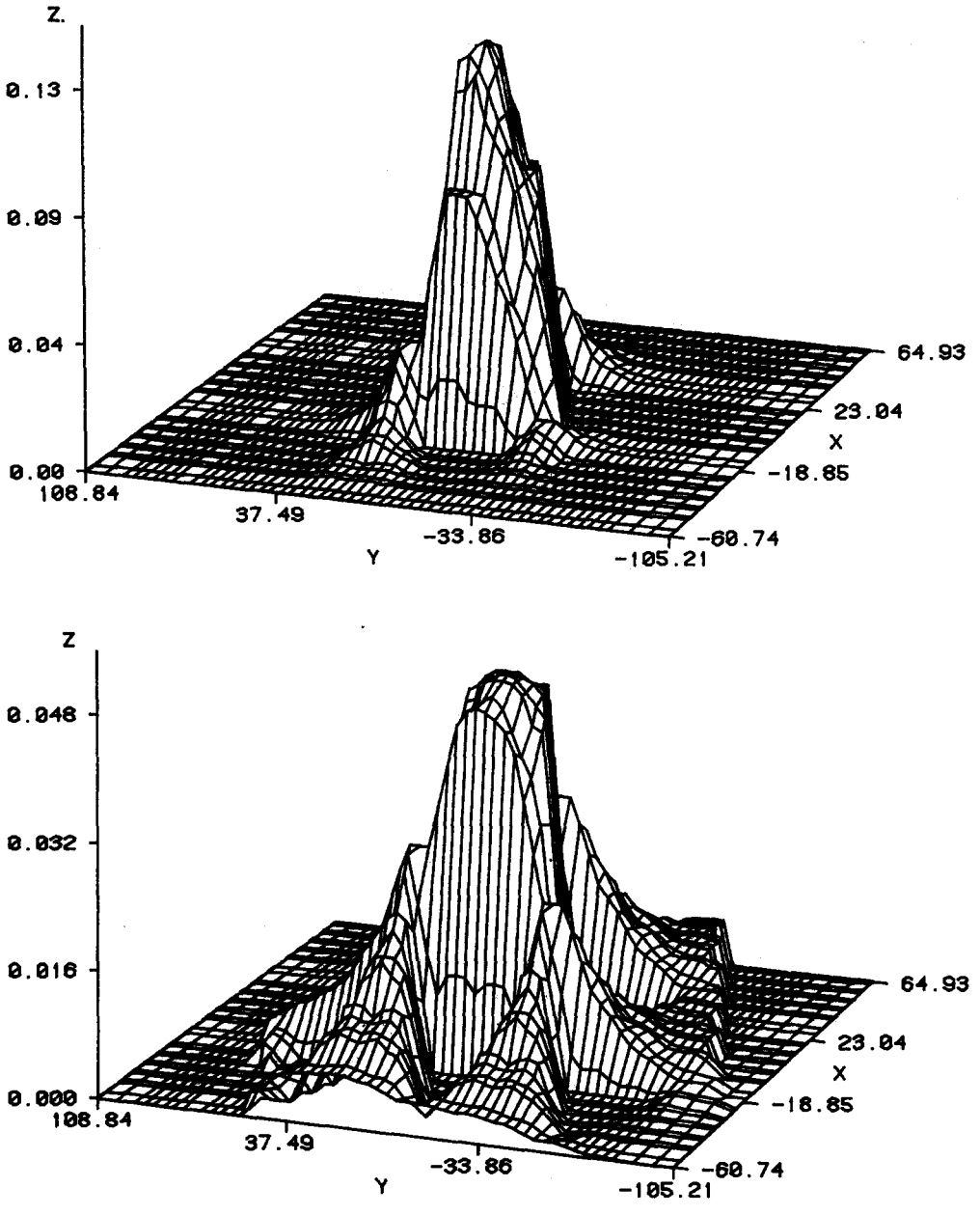

FIG. 6. Relative concentration of diffusion silicon atoms (plotted along the z-axis) as a function of time t and the surface coordinates. X and Y are the coordinates of the surface atoms shown in Fig. 1. The coordinates of point A of Fig. 1 are taken as (0,0) in this figure. (a) $t = 1000$ t.u.; (b) $t = 4000$ t.u. (1 t.u. $= 0.5 \times 10^{-7}$ s). Surface temperature is 1000 K.

The activation energy will be changed if the strength of the interaction between adatom and lattice is varied.

The Si–Si–Si bending frequency relevant to the surface diffusion case is not known from either experiment or *ab initio* theory. However, Raghavachari[25] has obtained a value of 206 cm^{-1} for this bending frequency from the results of MP4 calculations with 6-31G* basis sets. The semiempirical surface used by Gai, Thompson, and Raff[26] to study Si_3 trimer formation gives 193 cm^{-1} for this frequency. These results are about a factor of 2.5 larger than that given by the preexponential factor in the present calculations. Consequently, we might expect that more accurate representation of the Si–Si–Si bending forces on the surface could increase the preexponential factor by as much as a factor of 2–3.

The present potential assumes an Lennard–Jones (12,6) interaction between a lattice atom with a dangling bond and the adatom. The well-depth and equilibrium bond-length parameters, ϵ and r_0, for the pairwise interaction are 2.515 eV and 4.0 a.u., respectively. The interaction between the adatom and lattice atoms without dangling bonds is assumed to be repulsive and is obtained from the results of self-consistent-field (3-21G) calculations.[2] When all terms in the pairwise sums are included, the net *–Si bond energy is 2.31 eV. In contrast, semiempirical calculations on the gas-phase $H_3Si–SiH_2$ system yield a well depth and Si–Si bond length of 2.515 eV and 4.0 a.u., respectively.[27] Coltrin and co-workers[28] and Gordon, Truong, and Borderson[29] obtain a Si–Si equilibrium bond length of 4.5 a.u. for the H_3 Si–SiH system using *ab initio* methods at the MP4 level. Takai, Halicioglu, and Tiller[8] have taken the two-body Si–Si well depth parameter to be 2.817 eV and have used a value of 4.3 a.u. for the Si–Si equilibrium distance. NoorBatcha, Raff, and Thompson[6] have employed a Si–Si bond energy of 2.48 eV. The solid-phase, two-body Si–Si interaction parameters employed by Brenner and Garrison[30] are 2.1 eV and 4.4 a.u. for the bond energy and equilibrium distance, respectively. The

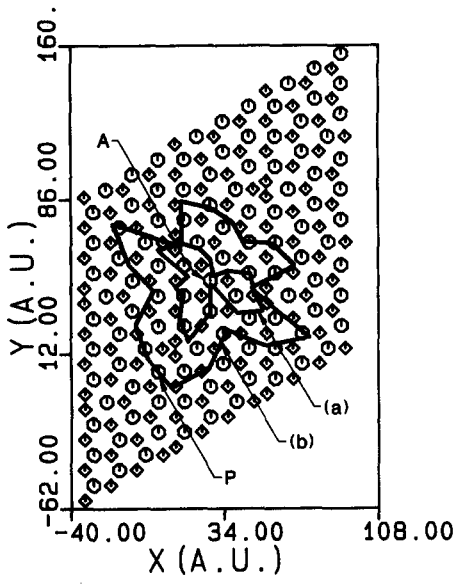

FIG. 7. Polar plot of the directional diffusion distance (DDD) as defined by Eq. (22) as a function of time t: (a) $t = 1000$ t.u.; (b) $t = 5000$ t.u. (1 t.u. $= 0.5 \times 10^{-7}$ s). Surface temperature is 1000 K. The octagonals and diamonds denote the surface atoms shown in Fig. 1.

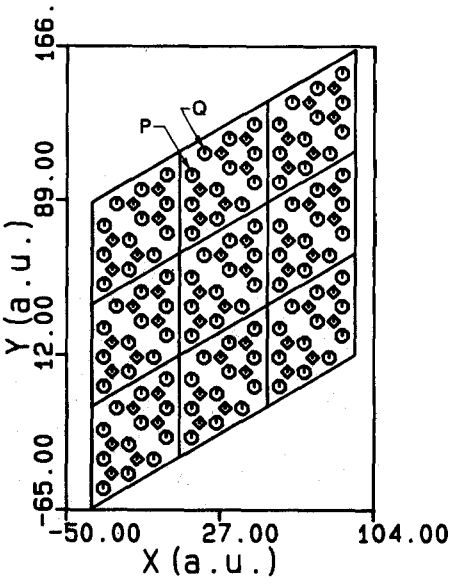

FIG. 8. Unrelaxed XY coordinates of 162 atoms with dangling bonds in nine unit cells of the Si(111)-(7×7) reconstructed surface model suggested by Takayanagi *et al.* Octagonals denote the 108 atoms in the top layer ($Z = 0$) and the diamonds represent the 54 atoms of the second layer ($Z = -1.48$ a.u.). The corresponding one atom per unit cell having a dangling bond in the fourth layer is not shown.

spread of these parameter values suggests that a more accurate evaluation of the adatom–lattice interaction in the Si(111)-(7×7) system may lead to different values for ϵ and r_0 in the semiempirical surface we have employed.

A crude estimate of the effect of such variations in the potential parameters can be made by considering the approximate change in the maximum of the minimum-energy path by exploring the region near the probable location of the barrier maximum for a stationary lattice. Such a study shows that a 10% increase in the value of ϵ in the present calculations would increase the activation energy by approximately the same fraction. This would result in a change in K_A and D by about a factor of exp (0.15 eV/$k_B T$), which has a value of 5.7 at 1000 K. The activation energy is a very sensitive function of r_0. An increase of 5% in r_0 might decrease the barrier by more than 0.3 eV, which would increase the diffusion coefficient at 1000 K by a factor of more than 32.5.

The interaction among the lattice atoms exerts a small effect upon the activation energy, e.g., a softer lattice potential that increases the vibrational amplitude of the lattice at a given energy would decrease the activation energy. However, this effect would be small. If, for example, a change in the lattice interaction produced a 0.1 a.u. increase in the vibrational amplitude, we estimate this would change the activation energy by about 0.1 eV.

The most significant change in the diffusion coefficient value would result from a change in the model used for the (7×7) reconstruction. For the Binnig *et al.*[20] model used in the present study, we have seen that although there are three distinct jump frequencies, K_A, K_E, and K_G, K_A is the rate-determining jump. However, in the dimer-adatom-stacking (DAS) model of the (7×7) reconstruction suggested by Takayanagi *et al.*[31] the situation is very different. The DAS model has 19 surface atoms per unit cell that have dangling bonds. Twelve of these are in the top layer, six are in the second layer, and one is in the fourth layer (see Fig. 8). An examination of this lattice indicates that while there are adjacent jumps that correspond to K_A in the Binnig *et al.* model, this jump rate would no longer be rate determining. This is because diffusion from one end of the unit cell to the other is not possible without jumping from a site such as P to one denoted by Q in Fig. 8. These lattice sites are at a distance of about 12.6 a.u. Consequently, we expect this jump to be the rate-determining step and the activation energy for diffusion to nearly equal that for the jump frequency $P \rightarrow Q$. A crude estimate based on the potential used for the Binnig *et al.* lattice suggests that the activation energy for diffusion on the DAS surface would be greater than 2.0 eV. Thus, the diffusion coefficient on the DAS surface would be smaller by a factor larger than exp (0.5 eV/$k_B T$), which is 331 at 1000 K. It would appear that very careful measurements of the temperature dependence of the diffusion coefficient on a Si(111)-(7×7) surface might determine which lattice model is the more likely to be correct.

ACKNOWLEDGMENTS

We are indebted to Dr. Betsy M. Rice for discussions of various aspects of the variational phase-space calculations. P.M.A. would like to thank Dr. Ramesh Sharda and his family for their hospitality during the course of this work. We are pleased to acknowledge financial support from the Air Force Office of Scientific Research under Grant No. AFOSR-89-0085. P.M.A. expresses his thanks to Vikram University, Ujjain, India, for granting him leave to pursue this research.

[1]P. M. Agrawal, D. L. Thompson, and L. M. Raff, Surf. Sci. **195**, 283 (1988).
[2]P. M. Agrawal, D. L. Thompson, and L. M. Raff, J. Chem. Phys. (to be published).
[3]J. Bloem and L. J. Giling, *Current Topics in Materials Science* edited by E. Kaldis (North-Holland, Amsterdam, 1978), Vol. 1, Chap. 4.
[4]J. M. Jasinski, B. S. Meyerson, and B. A. Scott, Annu. Rev. Phys. Chem. **38**, 109 (1987).
[5]I. NoorBatcha, L. M. Raff, and D. L. Thompson, J. Chem. Phys. **83**, 6009 (1985).
[6]I. NoorBatcha, L. M. Raff, and D. L. Thompson, J. Chem. Phys. **82**, 1543 (1985).
[7]I. NoorBatcha, L. M. Raff, and D. L. Thompson, J. Chem. Phys. **81**, 3715 (1984).
[8]T. Takai, T. Halicioglu, and W. A. Tiller, Surf. Sci. **164**, 327 (1985).
[9]R. F. C. Farrow, J. Electrochem. Soc. **121**, 899 (1974).
[10]R. C. Henderson and R. F. Helm, Surf. Sci. **30**, 310 (1972).
[11]H. C. Abbink, R. M. Broudy, and G. P. McCarthy, J. Appl. Phys. **39**, 4673 (1968).
[12]B. A. Joyce, R. R. Bradley, and G. R. Booker, Philos. Mag. **15**, 1167 (1967).
[13]J. C. Tully, G. H. Gilmer, and M. Shugard, J. Chem. Phys. **71**, 1630 (1979).
[14]B. M. Rice, L. M. Raff, and D. L. Thompson, J. Chem. Phys. **88**, 7221 (1988).
[15]J. D. Doll and H. K. McDowell, J. Chem. Phys. **77**, 479 (1982); H. K. McDowell and J. D. Doll, Surf. Sci. **121**, L537 (1982); J. D. Doll and H. K. McDowell, *ibid.* **123**, 99 (1982); H. K. McDowell and J. D. Doll, J. Chem. Phys. **78**, 3219 (1983); J. D. Doll, H. K. McDowell, and S. M. Valone, *ibid.* **78**, 5276 (1983).
[16]J. R. Banavar, M. H. Cohen, and R. Gromer, Surf. Sci. **107**, 113 (1981).
[17]S. M. Valone, A. F. Voter, and J. D. Doll, Surf. Sci. **155**, 687 (1985).
[18]J. G. Lauderdale and D. G. Truhlar, Surf. Sci. **164**, 558 (1985); J. Chem. Phys. **84**, 1843 (1986).
[19]R. Jacquet and W. H. Miller, J. Phys. Chem. **89**, 2139 (1985).
[20]G. Binnig, H. Rohrer, Ch. Gerber, and E. Weibel, Phys. Rev. Lett. **50**, 120 (1983); G. Binnig, H. Rohrer, F. Salvan, Ch. Gerber, and A. Baro, Surf. Sci. **157**, L373 (1985).
[21]P. N. Keating, Phys. Rev. **145**, 637 (1966).
[22]J. C. Keck, in *Advances in Chemical Physics*, edited by I. Prigogine, (Interscience, New York, 1967), Vol. XIII, p. 85.
[23]In principle, w must approach zero and the reflecting surface for the Markov walk should be far from the dividing surface, S_a. In practice, computational time considerations dictate that w be finite and that the reflecting surface be close to S'_a but at least a distance equal to the maximum step size beyond it. S'_a itself may be taken to be the outer reflecting surface provided w is equal to or greater than the maximum step size and upon reflection from S'_a, the phase-space point is recounted in the Monte Carlo sums in Eq. (15).
[24]L. M. Raff, I. NoorBatcha, and D. L. Thompson, J. Chem. Phys. **85**, 3081 (1986).
[25]K. Raghavachari, J. Chem. Phys. **83**, 3520 (1985).
[26]H. Gai, D. L. Thompson, and L. M. Raff, J. Chem. Phys. **88**, 156 (1988).
[27]L. W. Burggraf and L. P. Davis (private communication).
[28]P. Ho, M. E. Coltrin, J. S. Binkley, and C. F. Melius, J. Phys. Chem. **90**, 3399 (1986).
[29]M. S. Gordon, T. N. Truong, and E. K. Bonderson, J. Am. Chem. Soc. **108**, 1421 (1986).
[30]D. W. Brenner and B. J. Garrison, Phys. Rev. B **34**, 1304 (1986).
[31]K. Takayanagi, Y. Tanishiro, S. Takahashi, and M. Takahashi, Surf. Sci. **164**, 367 (1985); K. Takayanagi, Y. Tanishiro, M. Takahashi, and S. Takahashi, J. Vac. Sci. Technol. A **3**, 1502 (1985).